



Highly Efficient catalyst of TiO₂/chitosan for Photodegradation and Sonodegradation of Organic Pollutants

Robab Mohammadi *

Department of Chemistry, Payame Noor University, PO Box 19395-3697 Tehran, Iran

ARTICLE INFO

Article history:

Received 20 December 2021

Received in revised form 20 January 2022

Accepted 22 January 2022

Available online 22 January 2022

Keywords:

Sol-gel low-temperature

TiO₂/chitosan nanocomposite

Sonocatalysis

Photocatalysis

ABSTRACT

In the last decades, wastewater from the textile industry has become a major problem which leads to increase the concentration of pollution, which in turn represents environmental risks. The presence of dyes at even very low levels in effluent is highly visible and decomposition materials of these textile dyes are often carcinogenic. Due to the complex nature of synthetic dyes, conventional biological treatment processes are ineffective. Therefore there is a need of developing treatment methods that can lead to the complete degradation of the dye molecules from waste stream. Over the last few years, advanced oxidation processes (AOPs), especially sonocatalysis and photocatalysis, have proven to be effective processes for the wastewater treatment. The current study focused to develop a catalytic reactor via immobilized TiO₂ to degrade dyes in an effective method. In this research, TiO₂ nanoparticles prepared via sol-gel low-temperature method was successfully immobilized within chitosan and used as heterogeneous catalyst for the degradation of Acid Orange 7 (AO7) as an anionic dye. Transmission electron microscopy, scanning electron microscopy, and X-ray diffraction analysis were employed to characterize TiO₂/chitosan catalyst. Photodegradation and sonodegradation of AO7 by TiO₂/chitosan catalyst has been studied. XRD analysis indicated that prepared samples were 100% anatase phase and that chitosan interacted with TiO₂ nanoparticles and possessed good compatibility. TiO₂/chitosan nanocomposite showed high sonocatalytic and photocatalytic activities for the degradation of AO7. The rate constant of sonocatalysis was higher than that of photocatalysis. Sonocatalytic degradation of organic dye using prepared nanocomposite could be described by the mechanisms of hot spots and sonoluminescence. Furthermore, the photocatalytic degradation of AO7 via TiO₂/chitosan nanocomposite needs more time. Negative ΔG^0 and ΔH^0 values yielded from thermodynamic investigation proposed that the removal of AO7 via TiO₂/chitosan nanocomposite was simultaneous and exothermic in nature, respectively.

1. Introduction

The presence of organic pollutants in industrial wastewaters results in significant environmental contamination [1]. These wastewaters contain highly hazardous, carcinogenic and non-biodegradable that can cause harm to humans [2]. So, the removal of colored organic dyes from wastes is imperative. Up until now, different treatment methods have been developed for the degradation of pollutants, such as adsorption, chemical coagulation, filtration, sedimentation, and advance oxidation process (AOPs) [3-5]. Recently, AOPs are gaining significant attention because of their ability to

produce a sufficient number of highly reactive radicals for effective water decontamination. Among numerous AOPs, photocatalysis and sonocatalysis with metal oxide nanoparticles have attracted increasing attention as efficient methods for the removal of pollutants [4]. In the case of photocatalytic degradation, illumination with photon energy greater than the band gap of nanoparticles leads to the generation of electron and hole pairs, which can help in the formation of highly reactive oxygen species (ROS) that eventually participate in the decomposition of pollutants [6]. It is well known that the limiting parameter for catalytic decomposition depends upon the ability to generate

* Corresponding author. e-mail: Mohammadi_rb@yahoo.com

greater numbers of ROS [7]. Sonocatalytic decomposition of pollutants is caused via a chemical influence of ultrasonic (US) waves which arises from acoustic cavitation, i.e., generation, growth, and collapse of bubbles in a liquid [8]. The transient bubble collapse produces a localized hot spot with a very high temperature. Under such extreme conditions, thermal degradation of water takes place, resulting in the generation of highly reactive radical species, which can oxidize and decompose organic pollutants in water [9].

Semiconductor based photocatalysis technique is one of the most investigated procedures for the removal of pollutants [10]. Among various semiconductors, TiO_2 shows the most suitable properties: it is chemically and biologically inert, stable, non-toxic, cheap and easy to generate [9]. TiO_2 under UV light irradiation can generate oxidative (OH^\bullet) and reductive ($\text{O}_2^{\bullet-}$) species, which are able to remove various organic and inorganic compounds [5]. However, the obligation to separate the nanomaterials from the suspension after treatment restricts the process development. The above problems may be prevented via immobilization of the nanomaterials over appropriate supports [11]. The application of immobilized materials includes various benefits such as easy separation of the adsorbent, high adsorbent density and enhancing the retention of adsorbent in the reactor [12]. Chitosan is a natural polymer generated from brown algae, which has been widely employed in immobilization studies because of simple preparation, hydrophilicity and high adsorption potential to eliminate the pollutants [13]. Furthermore, adsorption capacity of the chitosan for sequestering anionic dyes because of the electrostatic attraction between the protonated amine groups on the chitosan and the sulfonic groups of the anionic dyes would be beneficial to increase the adsorption of anionic dyes together with the immobilized adsorbent [14].

The chemical applications of ultrasound, “sonochemistry” has shorter reaction times, is more likely to undergo a complete chemical reaction and more ordered crystallization. Sonochemistry is a procedure of cavitation that refers to the rapid growth and implosive collapse of bubbles in a liquid in an unusual reaction environment [15]. Sonocatalytic procedure, which is a combination of catalyst with ultrasonic has widely considered overcoming obstacles. Besides, the sonocatalytic performance to degrade organic pollutants can be enhanced because of a synergistic effect of ultrasonic illumination with a solid catalyst [16].

In recent decades, photocatalysis and sonocatalysis processes are considered as efficient methods for the elimination of pollutants. However, the comparative investigations of these processes are scarce in the literature. In order to detect if TiO_2 /chitosan nanocomposite can act as a sonocatalyst for removal of AO7, the present work focuses on the investigation and comparison of AO7 degrading in the sonocatalytic and

photocatalytic procedures.

The aim of the present study was to prepare TiO_2 /chitosan nanocomposite and evaluate its catalytic activity for the removal of an anionic dye (Acid Orange 7) from aqueous solutions. To find out which energy source is better in terms of the synergistic effect with TiO_2 /chitosan nanocomposite for the removal of dye, UV-C light and US waves were used as sources of energy. In addition, the photodegradation and sonodegradation mechanisms of AO7 on TiO_2 /chitosan nanocomposite were presented. The suggested mechanism of AO7 sonocatalytic degradation involves the sonochemical oxidation of AO7 molecules by $\text{OH}^\bullet/\text{HO}_2^\bullet$ radicals in solution and AO7 oxidation at the surface of TiO_2 /chitosan nanocomposite in the presence of O_2 activated by the cavitation event. These results are being compared herein with those of the photocatalytic AO7 degradation results.

2. Experimental

2.1. Materials

Titanium tetraisopropoxide (TTIP), glacial acetic acid (AcOH) and calcium chloride were purchased from Merck, Germany. AO7 were purchased from Alvan sabet company, Iran. Chitosan, which was of analytical grade, was purchased from Sigma-Aldrich.

2.2. Synthesis of TiO_2 nanopowders by sol-gel lowtemperature method in the presence of acetic acid under 0°C .

According to our previous work, in a flask kept in an ice/water bath, 3.78 g of acetic acid (AcOH) was mixed with 18.38 g of TTIP. Then, 220 mL of distilled water was added dropwise in about 30 min while stirring vigorously. The TTIP: AcOH: H_2O molar ratios were 1:1:200. The obtained sol—solution was kept in darkness for 12 h for nucleation procedure. Yielded solution was placed in an air oven at 70°C for gelation process. The gel was then dried at 100°C for overnight. The dry gel powder was calcined at 450°C for 3 h. [17].

2.3. Preparation of TiO_2 /chitosan nanocomposite

To prepare TiO_2 /chitosan nanocomposite, first chitosan (8 g) was dissolved in 1000 mL of 1 M acetic acid and then mixed via magnetic stirrer at 100 rpm for 2 h. TiO_2 nanoparticles (4 g) was added to the concentrated solution and mixed using magnetic stirrer for 1 h to reach homogeneity. The resulted mixture was kept for 8 h in a stable place. The weight ratio of chitosan to TiO_2 was 2:1. The mixture was added dropwise via a syringe to a mixture solution of NaOH (1.3 ml) and ethanol (20 ml). Then, they were stored in the solution for 24 h to allow the nanocomposite to be formed. The resulted sample was withdrawn from the solution and washed with deionized water several times to remove impurities. The obtained nanocomposite was dried in room temperature [18].

2.4 Characterization of prepared samples

The crystal phase composition and the size of synthesized materials were recorded via X-ray diffraction (XRD) (Siemens/D5000) with Cu K α radiation (0.15478 nm) in the 2 θ scan range of 10°–70°. The mean particle size (*D* in nm) was estimated by Scherrer's formula [19]:

$$D = \frac{k\lambda}{\beta \cos\theta} \quad (1)$$

where *k* is a constant equal to 0.89, λ , the wavelength of the X-ray equal to 0.154056 nm, β , the full width at half maximum intensity (FWHM) and θ , the half diffraction angle of the peak.

Size of the synthesized nanocomposite was measured via TEM instrument (Philips CM-10 HT-100 kV). The morphology of the synthesized nanocomposite was obtained by scanning electron microscope (SEM) (Philips XL-30ESM).

2.5 Studies and analysis

Removal of AO7 under UV irradiation was applied as a model reaction to investigate the photocatalytic and sonocatalytic activity of prepared samples. Photocatalytic removal investigations were carried out at atmospheric pressure in a batch quartz reactor. Artificial irradiation was supplied via 15W (UV-C) mercury lamp (Philips, Holland) emitted around 254 nm positioned above the batch photoreactor. In each test, 40 mg of catalyst and 20 mg L⁻¹ of AO7 were fed into the reactor and allowed to establish an adsorption–desorption equilibrium for 25 min in the darkness. The zero time reading was yielded from blank solution stored in the dark. While vigorous stirring, the reaction mixture was illuminated via UV light. The residual of AO7 was determined via UV-vis Perkin-Elmer 550 SE spectrophotometer at wavelength of 483 nm. Experimental set-up for the sonodegradation of AO7 via TiO₂/chitosan nanocomposite was similar to that of the photocatalytic removal of AO7. However, for the batch AO7 of AO7 via TiO₂/chitosan nanocomposite without light illumination, the set-up was exposed to sonication at ultrasonic power of 300 W. Pseudofirst order kinetics can be applied to describe the kinetic of the degradation rate of most organic dyes [20].

$$\frac{-dC}{dt} = k_{obs}C \quad (2)$$

In this equation, *k*_{obs} is the apparent rate constant which influenced via dye concentration. The following equation will be obtained via the integrating of this equation (with the same restriction of *C* = *C*₀ at *t* = 0):

$$\ln \frac{C_0}{C_t} = k_{obs}t \quad (3)$$

*k*_{obs} can be estimated from the plot of ln(*C*₀/*C*) versus *t*. The slope of this plot is equal to *k*_{obs}.

3. Results and discussion

3.1. Characterization of prepared samples

The XRD patterns of TiO₂ and TiO₂/chitosan samples are illustrated in Fig. 1 (a) and (b) respectively. The 2 θ peaks at 25.3° confirm the TiO₂ anatase structure without traces of the rutile and brookite phases (JCPDS card no 21–1272) [21]. From Fig. 1 (b), no chitosan crystal phase was detected in the XRD spectrum of TiO₂/chitosan nanocomposite. Therefore, the procedure of dispersion in chitosan has no effect on the crystal form of titanium dioxide nanopowders. However, the peak intensity was altered due to the H-bonding between chitosan and TiO₂ [22]. In general, the intensity of the diffraction peaks of TiO₂/chitosan is higher than that of TiO₂, indicating an increasing of crystallinity due to lattice distortion. The average size of crystallites for TiO₂ and TiO₂/chitosan detected from the XRD pattern based on the Scherrer's formula were about 10 and 8.3 nm, respectively. Smaller crystal size obtained for TiO₂/chitosan shows that chitosan is able to hinder the crystal growth of TiO₂.

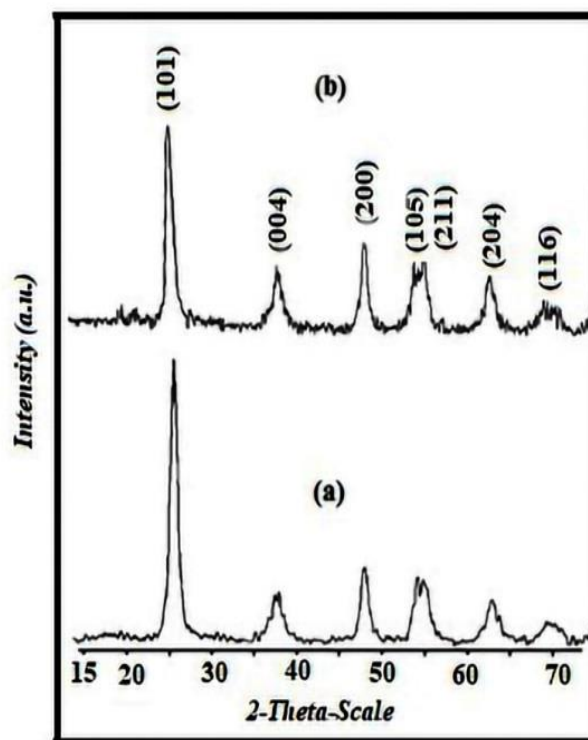


Figure 1. XRD patterns of (a) TiO₂ and (b) TiO₂/chitosan samples.

The morphology of TiO₂/chitosan sample was investigated by SEM (Fig. 2). The fine spherical nanostructures on surface for prepared sample can be seen from this figure. It can be concluded that chitosan is compatible with titanium dioxide nanoparticles. It is because of hydrogen bond formation between hydroxyl groups on the surface of titanium dioxide and chitosan [23]. Based on results, physical interaction, mainly hydrogen bonding, plays important role in binding the materials into the chitosan matrix. Also, highly porous structure of TiO₂/chitosan proposes the appropriate of the sample as an effective adsorbent for removal of AO7.

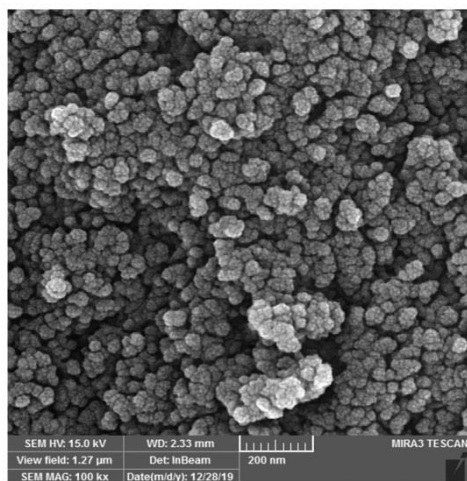


Figure 2. SEM image of TiO₂/chitosan nanocomposite.

TEM image of TiO₂/chitosan nanocomposite is shown in Fig. 3. The average size of the primary particles estimated from the TEM image is about 7–10 nm, which is in good agreement with that estimated from the XRD pattern via Scherrer equation. Chitosan layers on the titanium dioxide surface attached together and formed the porous structure. The porous structure can play a vital role in the specific interactions of nanocomposite with AO7 molecules.

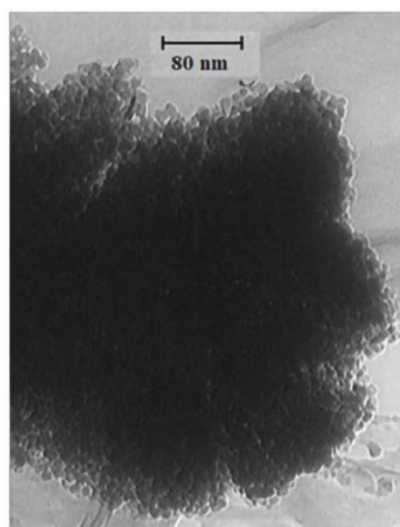


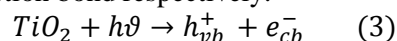
Figure 3. TEM image of TiO₂/chitosan nanocomposite.

3.2 Photodegradation of AO7 via synthesized samples

The results of photocatalytic removal of dye via prepared samples under UV illumination are presented in Fig. 4. It could be observed that the TiO₂/chitosan nanocomposite has more photocatalytic activity than TiO₂. The following mechanism would be proffered for the photocatalytic reactions [24].

a) When titanium dioxide is illuminated with UV light, electrons in the valence band are promoted to the conduction band. So, some holes and additional

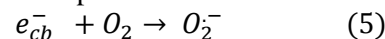
electrons are generated in the valence band and conduction band respectively.



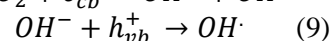
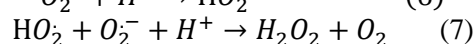
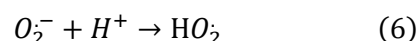
b) The positive charged hole may react with H₂O to generate OH[•].



c) The reaction between conduction-band electrons (e⁻) and proper electron acceptors (such as O₂) can generate Superoxide radicals.



d) Superoxide radicals can produce other species such as hydrogen peroxide (H₂O₂), hydroperoxy (HO₂[•]) and hydroxyl (OH[•]) radicals.



From Fig. 4, TiO₂/chitosan shows higher activity than titanium dioxide. Ti-OH groups in TiO₂ can incorporate with positively charged amino groups in the chitosan. It is well known that grafting of these functional groups is desirable for the adsorption of AO7 containing negatively charged sulfonated groups.

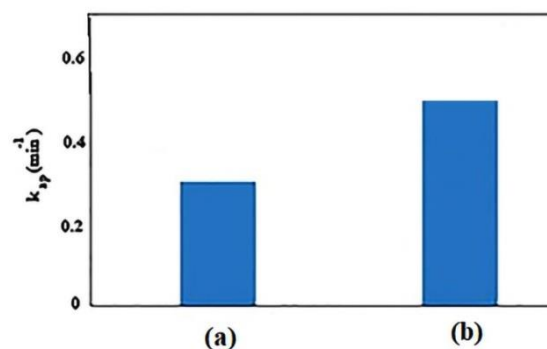


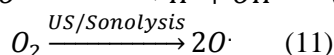
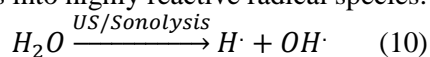
Figure 4. Photocatalytic degradation of AO7 in the presence of (a) TiO₂ and (b) TiO₂/chitosan samples.

3.3 Sonodegradation of AO7 via prepared samples

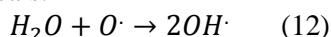
The degradation rate of AO7 was studied by exposing the pollutant solution to ultrasonication in the absence and in the presence of synthesized TiO₂/chitosan. AO7 undergoes negligible degradation under direct ultrasonic illumination in the absence of TiO₂/chitosan. This can be related to the low rate of OH[•] generation by sonolysis alone. Therefore, the presence of TiO₂/chitosan exhibited brilliant results as a sonocatalyst in the degradation of AO7 (Figure 5). This fact can be attributed to the increased number of cavitation bubble which occurs on the surface of TiO₂/chitosan and yielded in water cleavage and formation of excess OH[•]. Also, the fast degradation of AO7 by sonocatalytic procedure in the presence of TiO₂/chitosan is related to the sonoluminescence mechanism. Sonoluminescence

involves an intense UV-light, which promotes TiO₂/chitosan nanocomposite to act as an efficient photocatalyst during ultrasonic irradiation [25]. The sonodegradation mechanism of AO7 on TiO₂/chitosan can be explained as follows:

The chemical influences of ultrasound are because of the phenomenon of cavitation which is the nucleation, growth, and collapse of bubbles in a liquid [26]. The collapse of the bubbles induces high-energy phenomena, i.e., high temperature and pressure (~5000 K and 500 bars), electrical discharges, and plasma influences. The consequences of these extreme conditions are the direct thermal dissociation (sonolysis) of dissolved O₂ and H₂O molecules into highly reactive radical species:



These oxygen radicals can react with H₂O to generate hydroxyl radicals:



Based on researches, sonochemistry also involves the emission of light energy for a short period of time. The radiation can lead to the photoexcitation of electrons from the valence band to the conduction band, thus leading to the generation of electron-hole pairs in a similar manner as explained above for the photocatalysis [27]. OH[·] with high oxidizing activity can more react with AO7 and decompose it into small species. The organic pollutant decomposition mechanism included: (1) Adsorption, the electrostatic attraction between -NH₃⁺ group of chitosan and -SO₃⁻ of AO7 molecules; (2) sonocatalysis, the sonocatalytic degradation of pollutant via ultrasonic illumination began with excitation of TiO₂ and generation of electron-hole pairs. High oxidation valence-band holes (h⁺) can oxidize pollutant. Water decomposition or reaction of h⁺ with OH⁻ can generate OH[·]. Meanwhile, the reaction between conduction-band electrons (e⁻) and proper electron acceptors (such as O₂) yielded oxidative radicals. The generated OH[·] can easily degraded pollutant molecules [28].

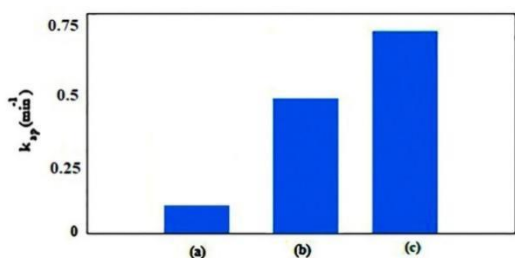


Figure 5. Sonocatalytic degradation of AO7 in the presence of (a) US only, (b) TiO₂, (c) TiO₂/chitosan samples.

3.4 Comparison of Efficiency of Photocatalysis and Sonocatalysis of TiO₂/chitosan nanocomposite

The degradation rate of AO7 by photolysis and sonolysis processes in the presence of TiO₂/chitosan nanocomposite is presented in Fig. 6. It can be seen that sonodegradation process is faster than photodegradation process. Therefore, US illumination is a better source than UV-visible illumination for the degradation of AO7 in the presence of TiO₂/chitosan nanocomposite.

TiO₂ nanoparticles have a lower band gap (3.2 eV). So, electron-hole recombination is faster and easier [29]. Therefore, the generation of hydroxyl radicals is difficult, which results in lower degradation of AO7 in the case of photocatalysis. In the presence of TiO₂/chitosan nanocomposite, the sonodegradation rate of dye was increased. This is because of synergistic effects of ultrasound and solid catalyst, namely [30], (i) added materials could provide additional nuclei for cavitation bubble generation, (ii) US illumination increases the mass transfer of AO7 between the liquid phase and TiO₂/chitosan surface, (iii) US illumination enhances the active surface area because of ultrasound disaggregating, and (iv) the catalyst can be promoted via ultrasound-induced luminescence which has a wide wavelength. This phenomenon can enhance the production of hydroxyl radicals in the reaction mixture [31]. Therefore, sonocatalysis can increase the degradation rate of dyes.

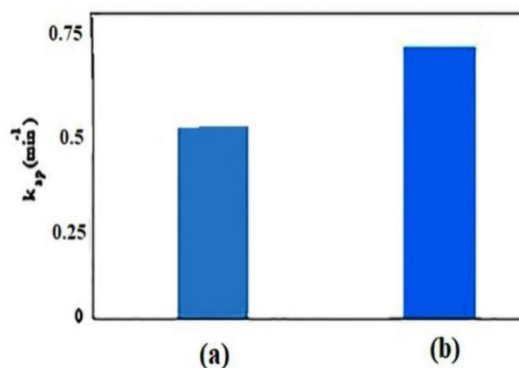


Figure 6. Degradation rates of AO7 under (a) UV-visible illumination and (b) US illumination.

3.5 Thermodynamic study

Temperature can influence physical and chemical reactions. In order to investigate the influence of temperature on catalytic degradation, standard enthalpy, standard entropy, and standard free energy, which may be obtained by Gibbs free energy equation, can be used to verify the characteristics of the catalytic process, such as whether it is endothermic/exothermic, spontaneous/nonspontaneous, and etc [32].

The thermodynamic investigation was performed by changing the solution temperature between 298 and 313 K. The free energy change or Gibbs free energy (ΔG^0) (kJ mol⁻¹), enthalpy change (ΔH^0) (kJ mol⁻¹) and entropy change (ΔS^0) (kJ mol⁻¹ K⁻¹) for the sonodegradation of AO7 by TiO₂/chitosan were estimated via Eqs. (10) and (11):

$$\Delta G^0 = -RT \ln K_D \quad (10)$$

$$\ln K_D = \left(\frac{\Delta S^0}{R} \right) - \left(\frac{\Delta H^0}{RT} \right) \quad (11)$$

where R, T (K) and K_D (q_e/C_e) are the universal gas constant, temperature and the distribution coefficient, respectively [23]. To study the thermodynamic of AO7 sonodegradation by TiO₂/chitosan nanocomposite, thermodynamic constants such as ΔG^0 , ΔH^0 and ΔS^0 were estimated by Eqs. (10) and (11). From the slope ($-\Delta H^0/R$) and intercept ($\Delta S^0/R$) of the plot of $\ln K_D$ versus $1/T$, the ΔH^0 and ΔS^0 were calculated, respectively (Fig. 7). The values of these factors are listed in Table 1. Table 1 demonstrates the negative ΔG^0 values, implying spontaneous nature of AO7 sonodegradation. A negative ΔH^0 implies an exothermic degradation procedure for AO7 pollutant. The negative value of ΔS^0 indicates the decline of degree of freedom of adsorbed AO7 on the binding sites of the catalyst at the solid–solution interface, indicating a strong binding of dye ions onto the active sites [33]. In agreement to the current study, Yakout et al. reported an exothermic, feasible and spontaneous process for Sono-sorption of crystal violet dye from aqueous solution by activated charcoal [33]. Jabeen et al. investigated degradation of Rhodamine-B dye via Pd/ZrO₂ catalyst, and found that the degradation process was spontaneous and exothermic [34].

A study focused on the sonodegradation of Acid Red 1 by zinc sulfide-titanium dioxide nanotubes (ZnS-TNTs) exhibited a behavior different from this trend. In order to investigate the effect of temperature on sonodegradation of Acid Red 1, experiments were conducted at 298-318 K. Interestingly, the value of enthalpy change was negative. This indicated that, the sonocatalysis process was endothermic [35].

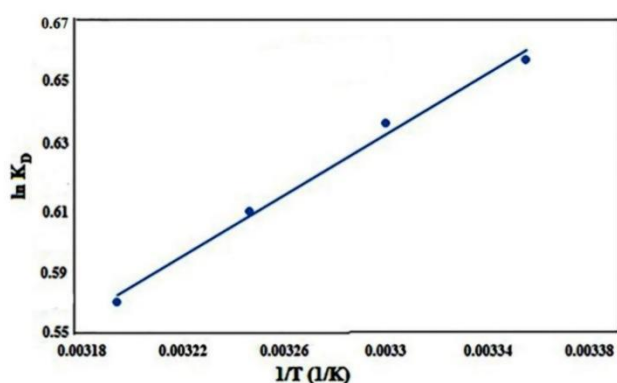


Figure 7. Thermodynamic profile for AO7 degradation by TiO₂/chitosan nanocomposite.

Table 1. Obtained parameters from thermodynamic study of AO7 degradation by TiO₂/chitosan nanocomposite.

Temperature (K) (ΔG^0) (kJ mol⁻¹) (ΔS^0) (kJmol⁻¹ K⁻¹) (ΔH^0) (kJ mol⁻¹)

298	-1.6	-0.0088	-4.19
303	-1.57	-	-
308	-1.54	-	-
313	-1.5	-	-

4. Conclusion

The present study was carried out to prepare and evaluate the efficiency of TiO₂/chitosan nanocomposite to photodegrade and sonodegrade an anionic dye (AO7) from aqueous solution. SEM analysis showed a highly porous structure for TiO₂/chitosan nanocomposite, which is suitable for sequestering dye molecules in aqueous solutions. The average size of the primary particles estimated from the TEM image was about 7–10 nm. The synergistic effect of TiO₂/chitosan nanocomposite and sonocatalysis has been demonstrated to be more effective in degrading AO7 as compared to TiO₂/chitosan nanocomposite and photocatalysis. Sonocatalytic degradation of AO7 in the presence of TiO₂/chitosan nanocomposite could be described via the mechanisms of hot spots and sonoluminescence. Furthermore, the photocatalytic degradation of AO7 via TiO₂ /chitosan nanocomposite needs more time. Overall, the application of TiO₂/chitosan nanocomposite can be a promising and efficient approach for the sonocatalysis of dyes. The results of thermodynamic investigation showed that the removal of AO7 by TiO₂ /chitosan nanocomposite is spontaneous and exothermic.

Acknowledgment

The author acknowledges the support of the Payame Noor University of Iran.

References

- [1] B. Neppolian, A. Bruno, C. L. Bianchi, M. Ashokkumar, Graphene oxide based Pt–TiO₂ photocatalyst: Ultrasound assisted synthesis, characterization and catalytic efficiency. *Ultrason. Sonochem.*, 19 (2012) 9–15.
- [2] N. Raghavan, S. Thangavel, G. Venugopal, Enhanced Photocatalytic Degradation of Methylene Blue Using ZnFe₂O₄ /MWCNT Composite Synthesized by Hydrothermal Method. *Mater. Sci. Semicond. Proces.*, 30 (2015) 321-329.
- [3] L. Parizot, T. Chave, M. E. Galvez, H. Dutilleul, P. Da Costa, S.I. Nikitenko, Sonocatalytic oxidation of EDTA in aqueous solutions over noble metal-free Co₃O₄/TiO₂ catalyst. *Appl. Catal. B Environ.*, 241 (2019) 570–577.
- [4] E. J. Park, J. Yi, K. H. Chung, D. Y. Ryu, J. Choi, K. Park, Oxidative stress and apoptosis induced by titanium dioxide nanoparticles in cultured BEAS-2B cells. *Toxicol. Lett.*, 180 (2008) 222-229.
- [4] S. B. Potdar, B. V. S. Praveen, S. H. Sonawane, Sonochemical approach for synthesis of zinc oxide-poly methyl methacrylate hybrid nanoparticles and its

- application in corrosion inhibition. *Ultrason. Sonochem.*, 68 (2020) 1–7.
- [5] J. Balachandramohan, T. Sivasankar, M. Sivakumar, Facile sonochemical synthesis of Ag₂O-guar gum nanocomposite as a visible light photocatalyst for the organic transformation reactions. *J. Hazard. Mater.*, 385 (2020) 121-129.
- [6] C. Zhong, X. Xiong, Preparation of a composite coating film via vapor induced phase separation for air purification and real-time bacteria photocatalytic inactivation, *Prog. Org. Coat.*, 161 (2021) 106486-106494.
- [7] J. A. Pinedo-Escobar, J. Fan, E. Moctezuma, C. Gomez-Solis, C. J. C. Martinez, E. Gracia-Espino, Nanoparticulate double-heterojunction photocatalysts comprising TiO₂ (Anatase)/WO₃/TiO₂ (Rutile) with enhanced photocatalytic activity toward the degradation of methyl orange under near-ultraviolet and visible light. *ACS. Omega.*, 6 (2021) 11840–11848.
- [8] R. Mohammadi, H. Eskandarloo, M. Mohammadi, Application of artificial neural network (ANN) for modeling of dyes decolorization by Sn/Zn-TiO₂ nanoparticles, *Desal. Wat. Treat.*, 55 (2015) 1922-1931.
- [9] A. Salma, H.V. Lutze, T.C. Schmidt, J. Tuerk, Photolytic degradation of the b-blocker nebivolol in aqueous solution. *Wat. Res.*, 116 (2017) 211 – 219.
- [10] H. Tibolla, J. T. Martins, F. M. Pelissari, E. M. Lanzoni, A. Vicente, Banana starch nanocomposite with cellulose nanofibers isolated from banana peel by enzymatic treatment :In vitro cytotoxicity assessment. *Carbohydr. Polym.*, 207 (2019) 169–179.
- [11] C. Wattanawikkam, W. Pecharapa, Structural studies and photocatalytic properties of Mn and Zn co-doping on TiO₂ prepared by single step sonochemical method. *Radiat. Phys. Chem.*, 2020 (171) 108714-108720.
- [12] K. Devagi, N. L. B. Ahmad, M. B. M. Sedik, T. Y. Guan, Y. Chin, Performance of solar photocatalysis and photo-fenton degradation of palm oil mill effluent. *Malays. J. Anal. Sci.*, 21 (2017) 996–1007.
- [13] A. F. Hassan, H. Elhadidy, Effect of Zr⁴⁺ doping on characteristics and sonocatalytic activity of TiO₂/carbon nanotubes composite catalyst for degradation of chlorpyrifos. *Phy. Chem. Solids.* 10 (2019) 13–25.
- [14] S. Mugundan, B. Rajamannan, G. Viruthagiri, N. Shanmugam, R. Gobi, P. Praveen, Synthesis and characterization of undoped and cobalt-doped TiO₂ nanoparticles via sol-gel technique. *Appl. Nanosci.*, 5 (2015) 449–456.
- [15] M. A. Fahad, S. Nouham, J. Mahjoub, G. Adel, E. Yassine, Populus tremula, Nerium oleander and Pergularia tomentosa seed fibers as sources of cellulose and lignin for the bio-sorption of methylene blue. *Int. J. Biol. Macromol.* 121 (2019) 655–665.
- [16] R. Mohammadi, B. Massoumi, B. Emamalinassabb, H. Eskandarloo, Cu-doped TiO₂-graphene/alginate nanocomposite for adsorption and photocatalytic degradation of methylene blue from aqueous solutions, *Desalin. Water. Treat.*, 82 (2017) 81-90.
- [17] M. Li, L. Gu, T. Li, S. Hao, F. Tan, D. Chen, D. Zhu, Y. Xu, C. Sun, Z. Yang, TiO₂-seeded hydrothermal growth of spherical BaTiO₃ nanocrystals for capacitor energy-storage application. *Crystals.*, 10 (2020) 1–15.
- [18] N. Kaur, G. Kaur, A. Bhalla, J. S. Dhau, G. R. Chaudhary, Metallosurfactant based Pd-Ni alloy nanoparticles as a proficient catalyst in the Mizoroki Heck coupling reaction, *Green. Chem.*, 20 (2018) 1506–15140.
- [19] R. Senthil Kumar, B. Gnanavel, High performance catalytic activity of pure and silver (Ag) doped TiO₂ nanoparticles by a novel microwave irradiation technique. *J. Mater. Sci. Mater. El.*, 28 (2017) 4253–4259.
- [20] H. Sutrisno, A. Ariswan, D. Purwaningsih, Effect of V dopant on physicochemical properties of vanadium-doped anatase synthesized via simple reflux technique. *J. Math. Fund. Sci.*, 48 (2016) 82–93.
- [21] S. R. abhajeet, R. K. Sonker, B. C. Yadav, Zn-Doped TiO₂ nanoparticles employed as room temperature liquefied petroleum gas sensor. *Adv. Sci.*, 10 (2018) 736–740.
- [22] R. Mohammadi, M. Mohammadib, Photocatalytic removal of methyl orange using Ag/Zn–TiO₂ nanoparticles prepared by different methods, *Desal. Wat. Treat.*, (2016), 57, 11317–11325.
- [23] S. E. Sharaf El-Deen, F. S. Zhang, Immobilization of TiO₂-nanoparticles on sewage sludge and their adsorption for cadmium removal from aqueous solutions. *J. Exp. Nanosc.*, 11 (2016), 239–258.
- [24] S. Rama Lingam, Synthesis of Nanosized Titanium Dioxide (TiO₂) by Sol-Gel Method. *Int. J. Innov. Technol. Explore. Eng.*, 9 (2019) 2278–3075.
- [25] R. Mohammadi, B. Massoumi, Sn/Cu-TiO₂ nanoparticles produced via sol-gel method: Synthesis, characterization, and photocatalytic activity, *Russ. J. Phys. Chem. A.*, 88 (2014) 1184–1190.
- [26] M. B. Suwarnkar, R. S. Dhabbe, A. N. Kadam, K. M. Garadkar, Enhanced photocatalytic activity of Ag doped TiO₂ nanoparticles synthesized by a microwave assisted method. *Ceram. Int.*, 40 (2014) 5489–5496.
- [27] R. Mohammadi, N. Sabourmoghaddam, Adsorption of azo dye methyl orange from aqueous solutions using TiO₂-SiO₂/alginate nanocomposite. *Asian. J. Green. Chem.*, 4 (2020) 107–120.
- [28] M. M. Karkare, Choice of precursor not affecting the size of anatase TiO₂ nanoparticles but affecting morphology under broader view. *Int. Nano. Lett.*, 4 (2014), 111-118.
- [29] B. Campanella, V. Palleschi, S. Legnaioli, Introduction to vibrational spectroscopies. *Chem. Texts.*, 7 (2021) 1–21.
- [30] L. Gonza´lez-Reyes, I. Hernández-Perez, L. Díaz-Barriga Arceo, H. Dorantes-Rosales, E. Arce-Estrada, R. Suarez-Parra, J.J. Cruz-Rivera, Temperature effects during Ostwald ripening on structural and bandgap properties of TiO₂ nanoparticles prepared by sonochemical synthesis, *Mater. Sci. Eng. B.*, 175 (2010) 9–13.
- [31] F.C. Robles Hernandez, L. Gonzalez-Reyes, I. Hernandez-Perez, Effect of coarsening of sonochemical synthesized anatase on BET surface characteristics, *Chem. Eng. Sci.*, 66 (2011) 721–728.
- [32] A. Déciga-Alcaraz, N. Delgado-Buenrostro, O. Ispanixtlahuatl-Meráz, Irreversible disruption of the cytoskeleton as induced by non-cytotoxic exposure to titanium dioxide nanoparticles in lung epithelial cells. *Chem. Bio. Int.*, 323 (2020) 109-24.
- [33] S. A. Ferraro, M. G. Domingo, A. Etcheverrito, D. G. Olmedo, D. R. Tasat Neurotoxicity mediated by oxidative stress caused by titanium dioxide nanoparticles

- in human neuroblastoma (SH-SY5Y) cells. *J. Trace Elem. Med. Biol.*, 57 (2020) 126413-126421.
- [34] S. Chakrabarti, D. Goyary, S. Karmakar, P. Chattopadhyay, Exploration of cytotoxic and genotoxic endpoints following subchronic oral exposure to titanium dioxide nanoparticles. *Toxicology and Industrial Health*, 35 (2019) 577-92.
- [35] F. H. Abdulrazzak, F. H. Hussein, A.F. Alkaim, I. Ivanova, V. Emeline, D. W. Bahnemann, Sonochemical/hydration-dehydration synthesis of Pt-TiO₂ NPs/decorated carbon nanotubes with enhanced photocatalytic hydrogen production activity. *Photochem. Photobiol. Sci.*, 15 (2016) 1347-1357.